Calibration of omnidirectional wave height spectra by SWIM through an BU-Net

Hailong Peng, Bo Mu, Danièle Hauser, Xiangjie Li, Hongling Ye, Ping Chen

Calibration of omnidirectional wave height spectra by SWIM through an BU-Net

Hailong Peng, Bo Mu, Danièle Hauser, *Senior Member, IEEE*, Xiangjie Li, Hongling Ye, Ping Chen, *Member, IEEE*,

***Abstract*—SWIM can provide global wave spectra, but under small sea conditions, the presence of parasitic peaks at low wavenumber, surfboard effects, and residual speckle noise lead to performance degradation of SWIM wave height spectrum products. To reduce the impacts of the factors above on SWIM wave height spectrum, in this paper, a convolution neural network (CNN) method based on BU-Net is proposed for calibrating SWIM omnidirectional wave height spectra with buoy measurements under sea states (wind wave mainly/swell mainly) and sea surface conditions (wind speed from 9m/s to 19m/s, significant wave height from 0.8m to 3.4m∼4.2m). The calibration results show that the impact of the factors above on SWIM omnidirectional wave height spectrum can be corrected. The correlation coefficients between the corrected SWIM beams 6°, 8°, 10 ° and the buoy mean omnidirectional wave height spectrum are all greater than 0.90, and the relative error of the peak wave number is within 10%. The relative error of the integrated energy is mostly less than 20%. In addition, the performance of spectral integration parameters (effective wave height H_s, energy wave period T_{m-10}) of each spectral beam of SWIM has been verified using MFWAM reanalysis data. The validation results show that RMSE of the H_s and T_{m-10}, for the corrected SWIM beam 6 ° (8 °, 10 °) under wind wave sea conditions are 0.31m (0.32m, 0.25m) and 0.50s (0.51s, 0.49s) respectively; those for swell cases are 0.16m (0.16m, 0.13m) and 0.87s (0.77s, 0.72s), respectively.**

***Index Terms*—omnidirectional wave height spectra, BU-Net, calibration, NDBC buoy.**

I. Introduction

OCEAN Waves play an important role in ocean engineering, navigation meteorology, ocean dynamics and other fields. The wave directional spectrum describes the change of wave energy with frequency and direction. The corresponding wave parameters, such as effective wave height, dominant or mean wavelength, and wave period, and dominant or mean wave direction, can be calculated on this basis. Therefore, the acquisition of wave directional spectrum is extremely important.

The directional spectrum of ocean waves is mainly obtained by field observation and microwave remote sensing. Buoys can provide the sea wave spectrum on a spot with a high accuracy. However, the number of buoy stations is very limited, and it is difficult to cover the whole world. In-situ wave observations also include waves visually observed from Voluntary Observing Ship (VOS), which provide long records of wave data, however, the wave records are somewhat subjective since the wave observation accuracies are based on the skill and experience of the observer. In addition to observational uncertainties, VOS-based wave climatologies suffer from inhomogeneous spatial and temporal sampling [1].

Satellite remote sensing can provide wave spectrum globally, also playing an important role in the wave observation system. SAR (Synthetic Aperture Radar) can provide wave spectra over the ocean, but with frequent smearing and distortion effects, in particular for waves shorter than about 200m when they propagate close to the along-track directions. This is due to the non-linear imaging mechanism associated with the velocity bunching effect [2], [3]. The wave scatterometer [4] is a RAR (Real Aperture Radar) system with a near-nadir scanning beam geometry, specially designed to measure the directional wave spectrum. Compared with SAR, wave scatterometer observations are not affected by the velocity bunching effect and are thus much less limited in the detection of wind waves. The wave scatterometer SWIM (Surface Waves Investigation and Monitoring) carried by CFOSAT (China France Oceanography Satellite) is the first space borne wave scatterometer [5], with which the world-wide directional spectra of ocean waves are produced systematically since the end of April 2019.

The research on SWIM wave spectrum performance verification has been carried out. Most studies [5], [6], [7], [8] verify the performance of SWIM wave spectrum products by comparing the wave parameters, including the significant wave height (SWH), peak wavelength, dominant wave direction, and angular spread of the dominant waves, calculated from the wave spectrum retrieved by SWIM and the wave parameters of the wave model reanalysis data. However, in these studies, the performance of the sea wave spectrum changing with the wave number cannot be verified since the sea wave parameters are only integral parameters of the sea wave spectrum. The comparison and verification of SWIM wave spectrum products and buoy measurement data are less,

This work was supported in part by National Key R&D program of China (No.2022YFC3104900/2022YFC3104901), in part by the National Natural Science Foundation of China under Grant 41976168, in part by the Shandong Joint Fund of National Natural Science Foundation of China under Grant U2006207. *(Corresponding author: Ping Chen)*

Hailong Peng and Bo Mu are with the National Satellite Ocean Application Service, Ministry of Natural Resources, Beijing 10081, China, also with the Key Laboratory of Space Ocean Remote Sensing and Application, Ministry of Natural Resources, Beijing 100081, China.

Danièle Hauser is with the Laboratoire Atmosphère, Milieux, Observations Spatiales (LATMOS), Université Paris-Saclay, UVSQ, Centre National de la Recherche Scientifique (CNRS), Sorbonne Université, 75005 Guyancourt, France.

Xiangjie Li, Hongling Ye, and Ping Chen are with the School of Electronic Information and Communications, Huazhong University of Science and Technology, Wuhan 430074, China(e-mail: chenping@hust.edu.cn)

mainly because it is difficult to obtain a sufficient number of SWIM-buoy space-time matching. To overcome this difficulty, a verification method without direct space-time matching was proposed [9]. The method is based on an assumption that for a given sea state condition (dominated by either wind sea or swell) and surface condition parameters (wind speed, wave age, significant wave height H_s and peak wavelength λ_p), the wave directional spectrum is independent of time and location. Based on mean spectra estimated for the same sea state classes and surface condition parameters, the SWIM wave spectral detailed properties were compared with those provided by buoy measurements [9], based on the analysis of the omnidirectional spectra and the angular distribution of wave energy at the spectral peak.

Their comparison [9] shows that SWIM data from beams 8° and 10° provide omnidirectional spectra in good agreement with buoy data as long as $H_s > 2.5$ m, with the correlation coefficient close to or higher than 0.90, the relative bias on energy ΔE within $\pm$ 20%, and the bias on the peak wave number Δk_p within $\pm$10%. For the same wave conditions, the results are not as good for the beam 6° where similar scores are reached only for $H_s > 3.5$m and significant slope $\delta < 0.03$.

The results [9] show that under small sea conditions ($H_s <$ 2.5 m), the precision of SWIM wave spectrum inversion decreases for all SWIM beams. It is because there is a kind of inherent parasitic peak at low wave number for the wave height spectrum inverted from SWIM, which is induced by the amplification of a noise floor of low energy remaining in the SWIM slope spectra but significantly amplified when these are converted to wave height spectra. Under large sea conditions, the parasitic peak is very small compared with the normal wave spectrum peak, so it will not affect the performance of wave spectrum inversion. However, for small sea conditions where the wave signal is weak, the false signal in low wave number becomes comparable or even larger than the wave signal, which leads to the overestimation of H_s obtained by the integral of the wave height spectrum by SWIM. This indicates the need to correct the wave spectra from this problem when converting wave slope to 1D wave height spectra.

From the results [9], another factor affecting the accuracy of SWIM wave spectrum inversion is the surfboard effect caused by a non-linear imaging mechanism [4], [9], [10], which becomes more significant when the incident angle is smaller or the sea slope is larger. The surfboard effect leads to that the peak of the wave energy containing part is shifted towards the low wavenumbers and is less energetic compared to the buoy spectrum.

In addition to the above-mentioned studies the validation and calibration of SWIM L2 off-nadir wave parameter data products has also been carried out in [11], [12], [13]. [11] uses the significant wave height measurement data of SWIM and other altimeters to calibrate the significant wave height data corresponding to the sea wave spectrum of SWIM L2 off-nadir data through a deep neural network (DNN). For the southern sea area of the South China Sea, [12] uses the data sets of two buoys in the sea area for two years to calibrate the dominant wavelength of SWIM based on the artificial neural network method. In [13], based on 21 months of NDBC buoy measurement data, an inversion model combining the significant wave height and wind speed obtained by SWIM nadir beam is established using the neural network method, and the average wave period data calculated by SWIM wave spectrum is calibrated with unprecedented accuracy.

However, at present, all the corrections or calibration of SWIM products are aimed at the integral parameters of the wave spectrum, not the wave spectrum itself. In this paper, based on the method to collect SWIM-buoy "matched" wave spectrum datasets proposed in [9], a convolution neural network (CNN) method based on BU-Net is presented to correct the SWIM omnidirectional wave height spectrum for the cases where the main wave component energy accounting for more than 90% of the total energy, by using the SWIM-buoy "matched" datasets. With such a correction, the parasitic peak at low wave number of SWIM wave height spectrum is effectively removed, and the influences of the surfboard effect on SWIM omnidirectional wave height spectra are reduced.

In section II, we introduce a method to obtain the dataset of SWIM-buoy by indirect space-time matching. Section III mainly introduces the SWIM omnidirectional wave height spectrum correction method based on BU-Net. Section IV gives the correction results obtained by the proposed correction method. The conclusions are drawn in section V.

II. SWIM-Buoy Matched omnidirectional wave height spectrum Datasets

In order to calibrate SWIM omnidirectional wave height spectrum with buoy data, we first need to obtain SWIM-buoy matched data pairs under the same sea surface conditions. Instead of carrying out a direct SWIM-buoy spatiotemporal matching, we choose here the method of [9]. We collect SWIM wave spectrum data and buoy spectrum data respectively under a given surface condition parameters (wind speed, significant wave height and peak wavelength). For the same couple of H_s and λ_p , the wave spectra may still correspond to different wave components (wind sea, swell conditions). In order to ensure that buoy data and SWIM data are compared under exactly the same sea surface conditions, only the conditions with a single wave component are further selected. Therefore, only the samples with the main wave component energy accounting for more than 90% of the total energy are selected. The method to separate data in either wind sea or swell categories here is described in section II-D.

When collecting buoy data that meet the requirements, in addition to the above sea surface conditions provided by the buoy data parameter, we also use the information on different wave partitions to select those samples with a relatively single wave component. Here, we analyze the MFWAM wave parameters of the different wave partitions and select conditions corresponding to a single wave component. Then, through a spatio-temporal matching of MFWAM and buoy data, we associate this pure wave component condition to the buoy data (see also section II-D). Similarly, by matching MFWAM and SWIM data, we apply the same method to select SWIM samples having only one wave component [9]. It is noted

that as the wind vectors are not provided in the MFWAM products, we take the wind vectors corresponding to each SWIM measurement from the "SWIM nadir_wind_box" data products.

In addition to sea states and sea surface conditions, ocean currents and rainfall can also affect the characteristics of omnidirectional wave spectra. We used the global sea surface current grid data of the Copernicus Marine Environment Monitoring Service (CMEMS) to remove data with ocean currents greater than 1 m/s, and used the Global Precipitation Measurement (GPM) product to remove rainfall data.

A. SWIM Data Set

CFOSAT SWIM is a Ku-band radar with a multi-incidence and scanning azimuthal geometry [5]. Off-nadir beams at 6°, 8°, 10° are called the "spectral beams", as observations from these beams are used for estimating the 2D wave spectra and wave spectra parameters. Each 2D spectrum is constructed from observations of successive overlapping antenna scans over 180° (on each side of the track), and representative of wave cells (boxes) of about 70×90 km.

The data products used in this paper are L1b and L2 SWIM products (version-5.1.2) from January 1, 2021 to September 30, 2021 provided by the China National Space Administration (CNSA). Using the rainfall information provided by GPM_3IMERGHH data product [14] and the sea land signs and sea ice coverage information provided by SWIM AUX data products, the rain free marine scene data are screened out from the SWIM data products. The data of strong current areas (speed>1 m/s) are also removed with daily surface currents provided by CMEMS , GLOBAL_ANALYSISFORECAST_PHY_CPL_001_015.

As intermediate products for the generation of wave spectra, L1b product provides radar cross section modulations, and modulation spectral density, impulse response function and speckle density spectrum, for each SWIM look direction and for the SWIM beams 6°, 8°, 10° [5], [15]. In this work, time and location from each macro-cycle in L1B products (i.e., from each sample in azimuth) are used for matching SWIM and MFWAM data.

The omnidirectional wave height spectrum data used in this article is not directly from the SWIM L2 data product. The wavenumber range of the omnidirectional wave height spectrum provided by the SWIM L2 data product has been truncated to 0.0126∼0.278 rad/m in order to reduce the impact of parasitic peaks at low wavenumber. Considering that wavenumber truncation will result in the loss of some information in the wave height spectrum, here the wavenumber range of $k_{min} = 0.0056$ to $k_{max} = 0.306$ rad/m are kept for the omnidirectional wave height spectra. In addition, L2 products provided with version-5.1.2 are wave slope spectra estimated using a Modulation Transfer Function (MTF) which forces the significant wave height H_s to be equal to the significant wave height provided by the nadir beam (this latter is estimated from the nadir waveform similar to altimeter missions, see [16]). However here, we go back to this initial version of the MTF because we are interested in calibrating the SWIM spectra in the version when their energy is not constrained by an additional information.

The wind speed information close to the position of the omnidirectional wave height spectrum is obtained from the variable named "nadir_wind_box" in the SWIM L2 nadir product. The nadir wind speed product have been verified to have a wind speed accuracy of 2 m/s [5].

B. NDBC buoy data

The buoy data used in this study come from NDBC buoy datasets provided by the National Oceanic and Atmosphere Administration (NOAA). The buoy parameters used here are wind speed, significant wave height, peak period, energy density spectrum $C_{11}(f)$ at 47 wave frequencies f from 0.02 Hz up to 0.4850 Hz [17].

Considering the influence of sea depth on wave spectrum, 49 NDBC buoy sites in deep water (water depth >200 m, distance from coastline >50km) were selected in this paper, and the time coverage was from January 2019 to September 2021.

In order to make the expression of spectral data consistent between NDBC and SWIM observations, it is necessary to transform the wave spectra from the buoy expressed as a function of frequency into wave height spectra expressed as a function of wave number. This is done by applying the dispersion relationship in deep water.

$$F(k) = C_{11}(f) / \left(\frac{8\pi^2 f}{g} \right). \tag{1}$$

where g is the gravitation acceleration.

In addition to converting the buoy spectrum into a wave number spectrum, a resampling is also applied in order to get the same sampling in wavenumber for both SWIM and buoy data: the buoy wave height density is linearly interpolated on a wavenumber grid k_i with a wavenumber interval of Δk over the wavenumber range (k_{min}, k_{max}). Here k_{min},k_{max} is set as the common measurement range of wave numbers by SWIM and buoy, i.e.,k_{min} =0.0056 and k_{max}=0.306 rad/m, and Δk is set as $k_{min}/10$. Thus, there are 536 wavenumber points for both SWIM and buoy omnidirectional wave height spectrum over the given wavenumber range. The peak wavenumber k_{p} in deep water for buoy data can be obtained with the peak period T_{p} according to

$$k_{\mathrm{p}} = \frac{4\pi^2}{T_p^2 g}. \tag{2}$$

C. MFWAM Data Set

The MFWAM is the French version of the third-generation wave model: the WAM model. It is based on the ECMWF version (referred to as ECW AMIFS-38R2) with a parameterization taken from the ST4 version of the WW3 model [18]. The MFWAM wave model takes into account the interaction between waves and ocean currents. The MFWAM wave model assimilates the significant wave heights and the spectral information from the spaceborne radar. The MFWAM wave model is driven by the wind field of the IFS-ECMWF

atmospheric system (with a time resolution of 3h) and its wave product has a grid size of 10km. The MFWAM reanalysis data product has a time resolution of 3h and a spatial resolution of 0.0833°×0.0833° (latitude and longitude). The MFWAM data products used here were downloaded from the Copernicus Marine Environment Monitoring Service (CMEMS).

The MFWAM data used in this paper are wave parameters of the total sea and of different wave components, namely, the most energetic swell (called 1^{st} swell), the second energetic swell (called 2^{nd} swell) and the wind waves. Three wave parameters of the total sea are used: significant wave height, peak wavelength and mean wave period.

D. Data Matchup and Sea State Classification

Firstly, SWIM sample of the L1B product (each macro cycle contained in a wave box [22]) is spatiotemporally matched with MFWAM to obtain the MFWAM wave parameters corresponding to each macro cycle. Then the MFWAM parameters of each SWIM macro cycle matched within a box of SWIM L2 product are averaged to obtain the collocated MFWAM data for this box. To avoid conditions of mixed seas for which the intercomparison results may be more difficult to interpret, the SWIM data with the main wave component energy accounting for more than 90% of the total energy are selected according to the partition parameters provided by MFWAM data.

Secondly, we matched spatiotemporally the MFWAM and buoy data (from January 2019 to September 2021) and then gather the buoy samples for each category relative to the different conditions according to buoy data, and finally we select those samples with the main wave component energy accounting for more than 90% of the total energy according to MFWAM partition data.

Thirdly, we need to classify the sea state and sea surface conditions. Wind wave sea and swell are considered as two main categories. Based on two parameters, a dimensionless height variance $\eta^* = \eta^2 g^2 / U_{10}^4$ and the inverse wave age $\Omega = \omega_p U_{10}/g$ as proposed by [19], [20], the samples with $\eta^* > 3.64 * 10^{-3}$, and $\Omega < 0.84$ are divided into pure swell category and those with $\eta^* \leq 3.64 * 10^{-3}$, and $\Omega > 0.84$ as pure wind waves category. In the above equations,η is the sea surface standard deviation ($\eta = H_s/4$) , ω_p is the peak angular frequency ($\omega_p = \sqrt{gk_p}$), g is the gravitational acceleration, H_s and k_p are respectively the total significant wave height and peak wave number provided by MFWAM in the above matching dataset.U_{10} is the wind speed at a height of 10m above the sea surface provided by SWIM, i. e., from (nadir_wind_box) of each geographic box in SWIM L2 data product.

Then different subcategories are defined. For wind wave sea, the samples are divided into subcategories in the wind speed range of 9 m/s-19 m/s with the center wind speed 10 m/s, 12 m/s, 14 m/s. . . .and a wind speed interval of 2 m/s. Then, within each of these subcategories, the data are analyzed according to different peak wavenumbers. Considering that the peak wave number provided by buoys are discrete values, while the peak wave number provided by SWIM and MFWAM are continuous values, here the center value of the peak wave number is set to the buoy wave number k_i, and its interval is set to $\left(\frac{k_{i-1}+k_i}{2}, \frac{k_i+k_{i+1}}{2}\right)$. where i is the ith wave number point.

As for the swell category, the samples are divided into subcategories in the significant wave height Hs range of 0.8 m-4.2 m with the center Hs 1 m, 1.4 m, 1.8 m. . . .and a height interval of 0.4m. In each of these subcategories, the data are classified according to the same subclass classification method for the wind wave case. In order to reduce the statistical fluctuation of buoy samples, only the subclasses with the buoy sample number larger than 50 are kept and used for the following calibration work.

We compared the mean omnidirectional wave height spectra of SWIM and NDBC buoys under different sea surface conditions using three evaluation indicators: relative error of integrated energy, relative error of peak wave number, and correlation coefficient. When the relative error of integrated energy is within 20%, the relative error of peak wave number is within 10%, and the correlation coefficient is greater than 0.95, it is considered that the SWIM omnidirectional wave height spectrum under the sea surface conditions is reliable and not corrected. According to this standard, as well as taking into account the continuity of sea surface conditions, for SWIM beams 6°, 8° and 10 ° , the sea surface conditions to be corrected are those H_s less than 4.2m (3.8m, 3.4m), respectively. Therefore, the subcategories for the pure wind wave (swell) case corresponding to the omnidirectional wave height spectrum data of the SWIM beams 6°, 8° and 10 ° to be corrected have 35, 34, and 33 subcategories (83, 81, and 72 subcategories), respectively.

For a sample set of each subcategory, we divide it into training set, and test set. Section III describes how to establish a calibration network based on the training set and in Section IV the performance of the calibration network is verified on the test set.

III. Method for calibration

Compared with the omnidirectional wave height spectrum measured by buoy, the omnidirectional wave height spectrum retrieved by SWIM has a nonlinear change due to the parasitic peak appearing at low wave number and the left shift and decrease of spectral peak caused by surfboard effect [10]. It is difficult to describe the complex nonlinear relationships between SWIM omnidirectional spectrum and buoy omnidirectional spectrum in an analytical manner. Therefore, it is difficult to correct SWIM spectrum by an analytical formula.

An artificial neural network (ANN) is a complex network structure formed by the interconnection of a large number of processing units (neurons). The network achieves the purpose of simulating the underlying complex relationship between input and output by repeatedly learning and training the known information and gradually adjusting the connection weight of neurons. Recently, ANN has been introduced into the field of ocean parameter correction, such as effective wave height, average wave period and other ocean wave parameter correction [11], [12], [13]. Considering that the omnidirectional wave spectrum has certain waveform characteristics, we adopt a

Convolution Neural Network (CNN) structure for calibration. CNN is widely used in image classification, image recognition, image segmentation and image denoising due to its outstanding feature extraction ability. U-Net, is a CNN originally used for medical cell segmentation. Later, U-Net is widely used in all directions of semantic segmentation (such as satellite image segmentation, industrial defect detection, etc.) due to its outstanding image feature extraction ability and segmentation effect. In addition, the BU-Net neural network, that is, adding a batch processing layer between the convolution layer and the activation layer, has been used in the study of ocean wave numerical model prediction and correction [21].

In this paper, an BU-Net neural network is used to correct SWIM omnidirectional wave height spectrum. In order to speed up the training speed of neural network and reduce the impact of internal parameter distribution deviation on the training of neural network, this paper uses BU-Net neural network architecture. Section III-A presents the BU-Net structure for calibration, while section III-B describes the method for data preprocessing and the method for training. Section III-C discusses the loss function with weights and trains the BU-Net network model.

A. BU-Net calibration modeling

Fig. 1 shows the structure diagram of SWIM omnidirectional wave height spectrum correction network model. The input and output of the network are SWIM uncorrected and corrected omnidirectional wave height spectrum, respectively. The network structure is based on BU-Net and is divided into an encoder and a decoder. As shown in Fig. 1, the encoder section includes a repeating structure that is composed of two convolutional layers(1×3), two batch normalization layers (BN, Batch Normalization), two activation layers, and one pooling layer. The length and width of the input and output of convolutional layers remain unchanged,and the number of convolution kernels determines the number of output channels. The BN layer is usually added right after the convolutional layer and before the activation function unit to accelerate the training process. Considering that the input omnidirectional wave height spectrum will have spectral value less than 0, in order to retain the negative feature of this part, the activation function in the encoder part uses leakyReLU [23]. The size of the convolution kernel is 1×3 and the stride is 1. Downsampling is achieved by maximum pooling, pooling size is 1×2 and stride is 1×2 so that the dimension of the image is halved. After each downsampling, the number of convolution kernels is doubled, and the above structure is repeated. The encoding processes on the left continuously compress the width of the feature. In the decoder section, upsampling is done by transposing convolution. After each upsampling, the number of convolution kernels is halved. The upsampled results are fused with the corresponding features of the encoder part, and then the convolution operation is carried out. The size and stride of the convolution kernel are consistent with the encoder part.The activation function of the decoder section is ReLU.

Three BU-Net models are established for SWIM beams 6°, 8°, 10 ° to calibrate SWIM omnidirectional wave height spectrum when Hs is 0.8m-4.2m, 0.8m-3.8m and 0.8m-3.4m, respectively.

B. Data preprocessing

To ensure equal opportunities for training SWIM samples under different sea surface conditions, 1) introduces a method to balance the sample size of SWIM under various sea surface conditions. 2) (respectively 3)) describes how we normalized the SWIM (respectively the NDBC buoy) omnidirectional wave height spectrum used in the BU-Net-based correction network.

1) Sample size balance: As mentioned above， there are different number of subcategories for a single wind wave case and a single swell wave case. In addition, the number of samples of SWIM omnidirectional wave height spectrum in each category for pure swell case is much larger than that of pure wind wave. Take the SWIM beam 6° as an example（the distribution of samples from SWIM beams 8 °and 10 ° are almost similar）, the average sample size of each subclass of pure swell is about 650, while the corresponding pure wind wave is 110. To ensure the equal sample number of each subcategory for both the wind wave and swell cases, the sample size of each wind wave subcategory is increased in the training set by repeating the wind wave sample operation. Moreover, the subcategory number for the wind wave case is increased by repeating wind wave subcategories several times. Through the sample balancing operation mentioned above, the neural network can equally learn the SWIM omnidirectional wave height spectra in training dataset under wind waves and swell cases.

2) Normalization of SWIM omnidirectional wave height spectrum: Under different sea conditions, the values of omnidirectional wave height spectra are quite different. This will lead to a large difference in the contribution of different subclass samples to the Loss function. This will affect the convergence of the neural network, so it is necessary to standardize the samples input to BU-Net. Here the omnidirectional wave height spectra of SWIM and buoy are standardized by using the nadir significant wave height (SWH) provided by SWIM L2 product, and the original data are transformed into standardized values with no dimension and no difference of the order of magnitude. The specific realization formula of standardization is as follows:

$$\mathrm{F'(k)} = \frac{\mathrm{F(k)}}{(\mathrm{H_{s\_nadir}}/4)^3}. \tag{3}$$

where $F(k)$ is the omnidirectional wave height spectrum measured by SWIM, $\mathrm{H_{s\_nadir}}$ is the nadir H_s of SWIM, and $\mathrm{F'(k)}$ is the normalized omnidirectional wave height spectrum.

3) Weighted normalization of the mean omnidirectional wave height spectrum of NDBC buoys: In order to train the BU-Net calibration model, the omnidirectional wave height spectra of buoy are used as the standard reference to correct the omnidirectional wave height spectra of SWIM. Since a single NDBC omnidirectional wave height spectrum sample

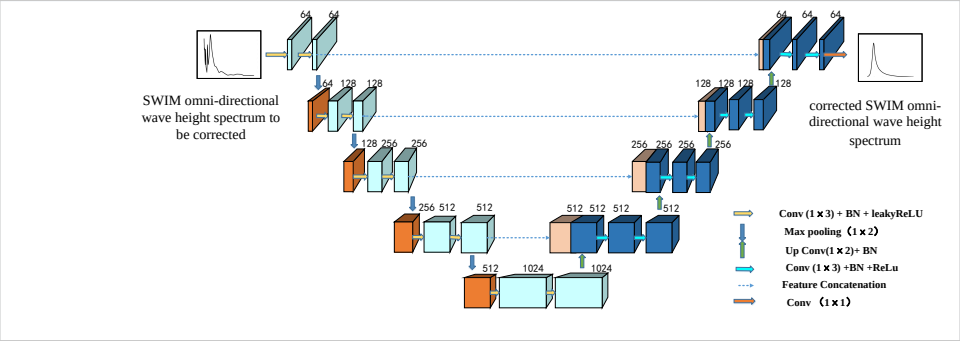

Fig. 1. Structure diagram of SWIM omnidirectional wave height spectrum correction network model.

has certain statistical fluctuations, firstly we carried out the spectrum average for buoy samples in each subcategory. A direct averaging of the spectral energy density may induce a reduction and/or broadening of the peak energy because the peak wave number may vary from one sample to another one. So we carried out the spectrum average by normalizing the wave number for buoy measurements with the same method described in [9]. Secondly, considering that each SWIM omnidirectional wave height spectrum in a given subcategory has its own H_s variability, one has to find the appropriate buoy reference spectrum corresponding to the SWIM sample. In output of the process, we want that the significant wave height of the corrected SWIM sample is consistent with reference values of H_s; here we consider that the MFWAM H_s spatiotemporally matched with each SWIM sample is the reference. A buoy sample label corresponding to the SWIM sample can be generated by using the following formula.

$$H_s^{buoy} = 4\sqrt{\sum_{i=1}^{N} F_{buoy}(k_i)\Delta k_i}. \tag{4}$$

$$F'_{buoy}(k) = \left(\frac{H_s^{MFWAM}}{H_s^{buoy}}\right)^2 F_{buoy}(k). \tag{5}$$

$$\tilde{F}'_{buoy}(k) = \frac{F'_{buoy}(k)}{(H_{s\_nadir}/4)^3}. \tag{6}$$

Where N is the point number of wave number, $F_{buoy}(\mathrm{k})$ is the mean buoy omnidirectional wave height spectrum for a subcategory, $\mathrm{H_s}^{\mathrm{MFWAM}}$ is MFWAM Hs with spatiotemporal matching with a SWIM sample; $F_{buoy}{}'(\mathrm{k})$ is NDBC buoy omnidirectional wave height spectrum weighted by significant wave height ratio, By (5), for each SWIM omnidirectional spectrum, the corresponding buoy label is $\tilde{\mathrm{F}}'_{\mathrm{buoy}}(\mathrm{k})$ with the significant wave height $\mathrm{H_s}^{\mathrm{MFWAM}}$. This is done to use the buoy spectral shape as the reference, while normalizing the total energy to the MFWAM model data. In (6), $\tilde{\mathrm{F}}'_{\mathrm{buoy}}(\mathrm{k})$ is a standardized $F'_{buoy}(k)$.

By using the above methods, the SWIM sample with different Hs in the same subclass can correspond to a different buoy sample label. Therefore, the established network based on such a dataset will be able to correct each individual SWIM sample.

Note that in the above steps, SWIM nadir H_s are used to normalize both SWIM and buoy sample, while MFWAM H_s is only used to weight buoy spectrum sample. Therefore, SWIM nadir H_s is easily accessible in operation, which need to be used in both training networks and using the established network, while MFWAM data is only used in training networks, and once the network is established, it does not need to be used.

C. Neural network training

The omnidirectional wave height spectra of SWIM beams 6 °, 8 ° and 10 ° will exhibit slightly different characteristics even under the same sea surface conditions. For example, under small sea conditions, the influence of parasitic peaks on the omnidirectional wave height spectra of beam 6 ° is greater than that of beams 8 ° and 10 °. Considering the above reason, we use different neural networks to correct the omnidirectional wave height spectra of SWIM beams 6 °, 8 °and 10 °, respectively.

The training of the BU-Net based correction network is carried out by MATLAB 2022b to run on NVIDIA TITAN X independent graphics card. The batch size was set to 256, the selected optimizer was “Adam”, the initial learning rate was set to 0.01. The Mini Batch Stochastic Gradient Descent (Mini Batch SGD) algorithm is used for network model training. The training set randomly shuffles the sample order every time it is learned, with a batch size of 256, and the L2 regularization was used to prevent overfitting.The super parameter of LeakyReLU Activation function of encoder part of each beam network model α is set to 0.01, α represents the slope of the activation function when the input data is less than 0.

The omnidirectional wave height spectrum is also affected by residual speckle noise at high wavenumbers, resulting in poor consistency with the reference spectrum at high wavenumbers. Usually the omnidirectional wave height spectrum value at the high wave number is small, thus a penalty term is added to the Loss function to increase the penalty at the high wave number. The weighted Loss function with the partial aggravation punishment at high wave number is as follows:

$$Loss_{weighted} = \frac{1}{M}\sum_{i=1}^{M}\sum_{j=1}^{N} w_{ij}\left[\tilde{F}_{out\_i}(k_j) - \tilde{F}'_{buoy\_i}(k_j)\right]^2. \tag{7}$$

where

$$w_{ij} = \begin{cases} a_1, \eta_i^* \leq 0.00364 \cup k_j > 2k_{p_i} \\ a_2, \eta_i^* > 0.00364 \cup k_j > 2k_{p_i} \end{cases}. \quad (8)$$

Where M is the batch size, set as 256; N is the number of wavenumber points in the unified wavenumber domain (0.0056,0.306); $\mathrm{k_j}$ is the jth wavenumber point in the unified wavenumber domain; $\mathrm{k_{p_i}}$ the peak wave number of the reference spectrum corresponding to the ith SWIM omnidirectional wave height spectrum to be corrected in a batch of samples; $\tilde{\mathrm{F}}_{\mathrm{out\_i}}(\mathrm{k})$ is the ith SWIM omnidirectional wave height spectrum corrected by a neural network model in a batch; $\tilde{\mathrm{F}}'_{\mathrm{buoy\_i}}(\mathrm{k})$ the reference spectrum corresponding to the ith SWIM omnidirectional wave height spectrum; η_{i}^* the dimensionless variance corresponding to the ith uncorrected spectrum in a batch; ω_{ij} is the penalty coefficient based on sea conditions and the difference between wave number and peak wave number, a_1 and a_2 is the penalty coefficient for the high wave number part of SWIM omnidirectional wave height spectrum for the wind wave case and swell case, respectively.

During network model training when the loss function of the SWIM beams 6 °, 8 ° and 10 ° respectively no longer decreases, and there is no overfitting or underfitting, then the corresponding correction network model training is completed. We adjust the penalty coefficient a_1 and a_2 in a range of 0-15, observe the training results, and then determine the relevant parameters of the network model. The Learning rate, iteration times (recorded with epoch) and penalty coefficient a_1 and a_2 finally determined for a correction network for SWIM beam 6 ° (8 ° and 10 °) omni-directional wave height spectrum are shown in Table 1 below:

TABLE I
RELEVANT PARAMETERS OF SWIM 6 °, 8 °, AND 10 ° OMNIDIRECTIONAL WAVE HEIGHT CORRECTION NETWORK MODEL

Beam （°）	Learning rate	iteration times （epoch）)	a_1	a_2
6	0.01	135	8	10
8	0.01	68	8	8
10	0.01	102	8	8

IV. CALIBRATION RESULTS

Once the calibration network is established, one can use it to calibrate the SWIM omnidirectional wave height spectrum. Below, we will verify the correction effect of the calibration network through the test dataset. Firstly, the samples of SWIM omnidirectional wave height spectra from test datasets are normalized by using H_s provided by SWIM L2 nadir product, secondly the normalized omnidirectional wave height spectra sorted into wind wave and swell subcategories for each set of SWIM data at 6°, 8° and 10° are input into the corresponding calibration network, thirdly, the output of the calibration network is denormalized also by SWIM nadir H_s to obtain the corrected SWIM omnidirectional wave height spectrum. Furthermore one can calculate the corresponding spectral parameters of the corrected samples. Section IV-A mainly compares SWIM mean omnidirectional wave height spectra before and after correction with the mean buoy spectra, while Section IV-B compares SWIM integral spectral parameters before and after correction with those provided by MFWAM reanalyzed data.

A. Omnidirectional wave height spectrum results

As described in section III-B, in the same subcategory, each uncorrected SWIM omnidirectional wave height spectrum sample is different, and the corresponding label buoy omnidirectional spectrum of each sample is also different. The established network corrects for each individual sample, so the corrected SWIM omnidirectional wave height spectrum in a subcategory is with certain statistical fluctuations. In order to reduce the fluctuations and compare the SWIM omnidirectional spectrum with the buoy omnidirectional spectrum more clearly, the SWIM omnidirectional spectra of the same subcategory are averaged using the same method as in [9], i.e., after applying a normalizing procedure on the wave numbers, in order to avoid a reduction or broadening of the peak energy due to fluctuations of the peak position between samples (see [9]). Then, we compare the mean omnidirectional wave height spectrum estimated from SWIM before and after correction and from buoys under corresponding sea surface conditions.

In order to quantitatively analyze the correction effect of omnidirectional wave height spectrum, the correlation coefficient, integrated energy error, and relative error of peak wave number are used. The correlation coefficient CC represents the degree of correlation between the mean SWIM and buoy omnidirectional wave height spectrum. CC is calculated as follows:

$$CC = \frac{\sum_{i=1}^{N}[\bar{F}(k_i) - \mu_A][F_{buoy}(k_i) - \mu_B]}{\sqrt{(\sum_{i=1}^{N}[\bar{F}(k_i) - \mu_A]^2)(\sum_{i=1}^{N}[F_{buoy}(k_i) - \mu_B]^2)}}. \quad (9)$$

Where N is the point number of wave number, $\bar{F}(k_i)$ and $F_{buoy}(k_i)$ are the mean SWIM and buoy omnidirectional wave height spectrum in the same sea-state class; μ_A,μ_B represent the mean of $\bar{F}(k_i)$ and $F_{buoy}(k_i)$, respectively.

The relative error of integrated energy $\Delta\mathrm{E}$ is used to quantitatively describe the energy difference between the SWIM and buoy mean omnidirectional wave height spectrum. The closer the absolute value of ΔE is to 0, the smaller the energy difference between the two mean omnidirectional wave height spectra. The calculated integral energy error is as follows:

$$\Delta E = \frac{\sum_{i=1}^{N} \bar{F}(k_i)\Delta k_i - \sum_{i=1}^{N} F_{buoy}(k_i)\Delta k_i}{\sum_{i=1}^{N} F_{buoy}(k_i)\Delta k_i} \times 100\%. \quad (10)$$

Where Δk_i is equal wavenumber intervals on a unified wavenumber domain.

Relative error of peak wavenumber Δk_p is defined as:

$$\Delta k_p = \frac{k_{p\_SWIM} - k_{p\_buoy}}{k_{p\_buoy}} \times 100\%. \quad (11)$$

Where $\mathrm{k_{p\_SWIM}}$ and $\mathrm{k_{p\_buoy}}$ are the peak wave number from the SWIM and buoy mean omnidirectional wave height spectrum.

1) Corrected SWIM omnidirectional wave height spectrum for the pure wind wave: Fig.2 compares the SWIM mean omnidirectional wave height spectrum before and after correction with the mean buoy spectrum, for the pure wind wave case. Fig.2 (a-d-g-j-m-p), (b-e-h-k-n-q), and (c-f-i-l-o-r) correspond to the comparison results of SWIM 6 °, 8 ° and 10 °beams, respectively. Fig.2 (a-b-c-d-e-f) correspond to the growing wind waves ($\Omega = 1.3$) with wind speeds of 10, 12, 14, 16, and 18m/s, while Fig.2 (g-h-i-j-k-l) and (m-n-o-p-q-r) correspond to the mature wind waves ($\Omega = 1$) and fully grown wind waves ($\Omega = 0.84$) with wind speeds of 10, 12, 14, and 16m/s. The solid line in the figure represents the buoy mean omnidirectional wave height spectrum, while the dotted line and the dashed lines represent the SWIM mean omnidirectional wave height spectrum before and after correction, respectively. The legend indicates the number of NDBC buoy samples corresponding to each subclass, as well as CC ,ΔE, and Δk_p. The performance evaluation parameters will be further discussed in Fig.3.

It can be seen in Fig.2 that for wind speeds smaller than 14m/s, the SWIM mean omnidirectional wave height spectrum before correction (dotted lines in the panels of Fig.2) has parasitic peaks at low wave numbers. The smaller the wind speed, the greater the impact of the parasitic peaks. An abnormal uplift of the energy level at low wave numbers is also evident at high wind speeds for developing and mature wind waves in Fig.2 (a-b-c-d-e-f) and Fig.2 (g-h-i-j-k-l), respectively. In addition, for wind speeds smaller than 14m/s, compared with the buoy mean omnidirectional wave height spectrum, most of the SWIM mean omnidirectional wave height spectrum before correction has a lower spectral peak, and the peak wave number deviates to the left ($\Delta \mathrm{kp} < 0$), which is attributed to the surfboard effect [9], [10]. In opposite, in the corrected SWIM mean omnidirectional wave height spectra (dashed lines in the panels of Fig.2), the parasitic peak at low wave number disappears, compared with those before correction. The phenomena that the energy at the peak is underestimated and that the peak wave number shifts to the left (likely due to the surfboard effect) are also reduced.

In order to better illustrate the correction effect for SWIM omnidirectional wave height spectra for the pure wind wave case, Fig.3 shows the evaluation indicators before and after correction for SWIM beams 6 °, 8 ° and 10 °. The horizontal axis represents the evaluation index before correction, and the vertical axis represents the evaluation index after correction. Fig.3 (a-b-c), (d-e-f), and (g-h-i) show the correlation coefficients, integral energy errors, and relative errors in peak wavenumber, respectively. Fig.3 (a-d-g), (b-e-h), and (c-f-i) show the distribution of evaluation indicators at beams 6 °, 8 °, and 10 °, respectively. In the subgraph, the solid red line represents y=x.

From Fig.3 (a-b-c), it can be seen that for the pure wind wave case, the correlation coefficients of the corrected mean omnidirectional wave height spectra of SWIM beams 6°, 8° and 10 ° are all greater than 0.9, indicating a significant improvement compared to the correlation coefficients before correction. Fig.3 (d-e-f) shows that the absolute values of $\Delta\mathbf{E}$ in the mean omnidirectional wave height spectra of SWIM beams 6 ° and 10 ° after correction are both less than 20%. The absolute values of $\Delta\mathbf{E}$ for SWIM beam 8 ° after correction are only greater than 20% when the peak wavenumber is 0.13 rad/m and the wind speed is 12 m/s. Although the absolute values of $\Delta\mathbf{E}$ are greater than 20% at this time, they are still better than before correction. Fig.3 (g-h-i) shows the absolute values of Δk_p are all less than 10%.

2) Corrected SWIM omnidirectional wave height spectrum for the pure swell case: This section selects swell conditions with peak wavelengths of 200, 300, and 400 m, demonstrates the correction effect of the correction network model in the SWIM omnidirectional wave height spectrum for the pure swell condition.

Fig.4 shows the comparison between the mean omnidirectional wave height spectrum before and after SWIM correction and buoy spectrum, for swell cases. Fig.4 (a-b-c-d-e-f), (g-h-i-j-k-l), and (m-n-o-p-q-r) correspond to $k_p = 0.0157rad/m,\ k_p = 0.0211rad/m$ and $k_p = 0.0308rad/m$, respectively. Due to the narrow spectral shape for the pure swell case, in order to clearly observe the difference in SWIM omnidirectional wave height spectrum before and after correction, Fig.4 only shows the spectrum part with wave numbers in the range of 0.0056∼0.125 rad/m.

From Fig.4, it can be seen that when $k_p = 0.0211rad/m$ and $k_p = 0.0308rad/m$, the uncorrected SWIM mean omnidirectional wave height spectrum is affected by parasitic peaks, and the smaller the effective wave height, the more obvious the influence of these parasitic peaks. The mean omnidirectional spectral of each SWIM beam before correction in Fig.4 (except case of $k_p = 0.0308rad/m$,$H_s = 2.2m$ in Fig.4 (r))is higher than that from the buoys at the peak wavenumber and when the wave number is greater than the peak wave number (high wave number part). After correction, the parasitic peak of the SWIM mean omnidirectional wave height spectrum disappears, and the difference in spectral values at the peak wavenumber and high wavenumber decreases, compared with the buoy spectrum.

In order to better illustrate the correction effect of SWIM omnidirectional wave height spectrum for the pure swell case, Fig.5 compares the evaluation indicators before and after correction for SWIM beams 6 °, 8 °and 10 °. The subfigures in the figure is the same as Fig.3 but for the swell cases.

From Fig.5 (a-b-c), it can be seen that the absolute correlation coefficients between the corrected SWIM omnidirectional wave height spectrum and buoy spectrum are all greater than 0.9. Fig.5 (d-e-f) shows that for the pure swell case, the absolute values of ΔE in the mean omnidirectional wave height spectrum of the corrected SWIM spectral beams are mostly smaller than the absolute values of ΔE before correction. Among them, the maximum absolute values of ΔE in the corrected SWIM beams 6°, 8°, and 10 ° are 14.8%, 18.1%, and 10.1%, respectively. From Fig.5 (g-h-i), it can be seen that the maximum absolute values of $\Delta \mathrm{k_p}$ decreases from 25.9%, 18.7%, and 20.7% for the uncorrected, to 9.7%, 7.7%, and 10.1% for the corrected, for SWIM beams 6°, 8° and 10 ° , respectively. It can be seen that the correction provided by the NN model to the SWIM omnidirectional wave height spectrum

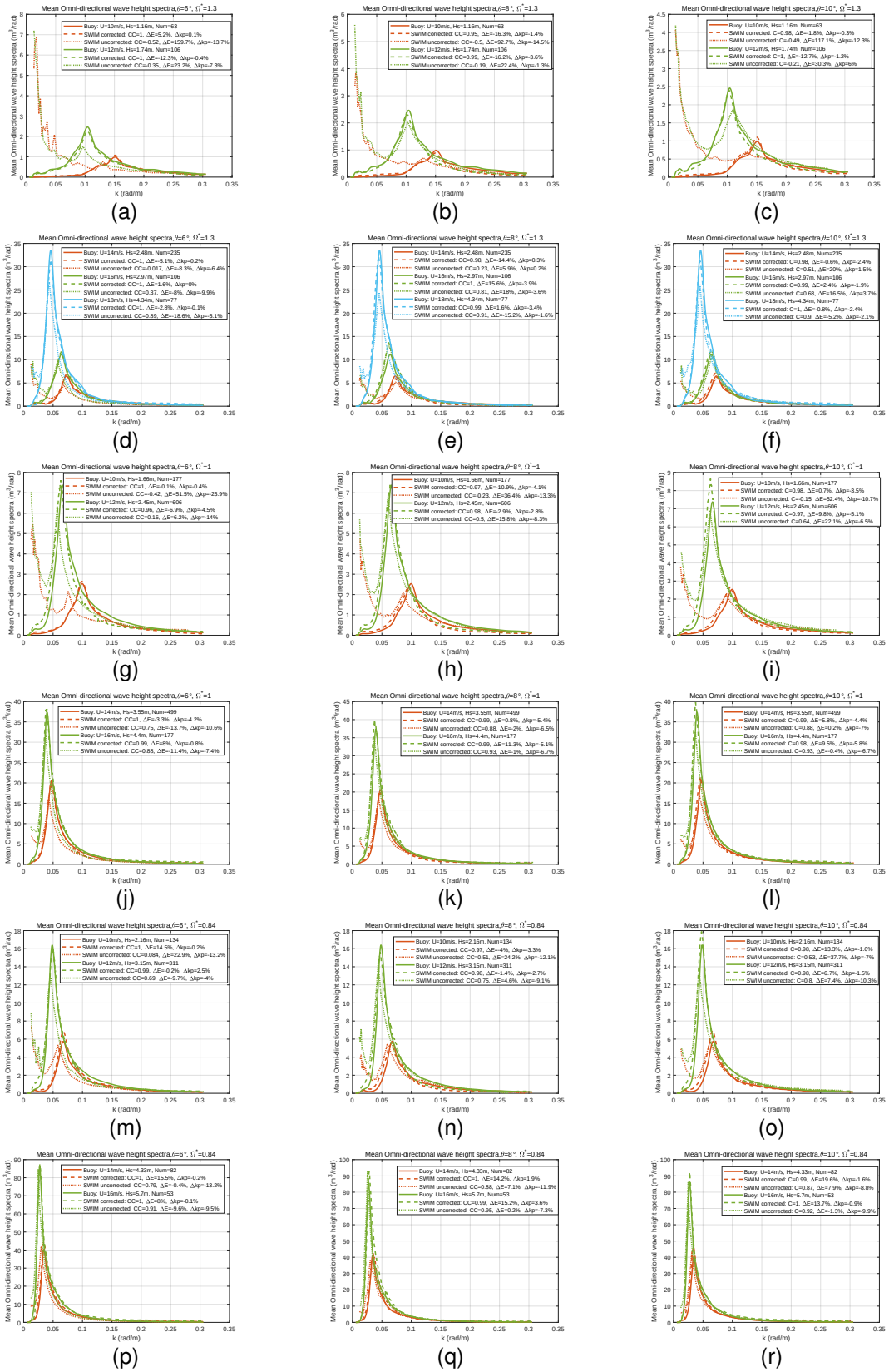

Fig. 2. comparison of the mean omnidirectional wave height spectra of SWIM and buoys before (dotted lines) and after (dashed lines) correction for the pure wind wave case, including growing wave $\Omega = 1.3$ (a-b-c-d-e-f), mature wave $\Omega = 1$ (g-h-i-j-k-l), and fully grown wave $\Omega = 0.84$ (m-n-o-p-q-r). The red and green lines in Fig.2 (a-b-c-g-h-i-m-n-o) represent wind speeds of 10m/s and 12m/s, respectively. The red, green, and blue lines in Fig.2 (d-e-f) represent wind speeds of 14m/s, 16m/s, and 18m/s, respectively. The red and green lines in Fig.2 (j-k-l-p-q-r) represent wind speeds of 14m/s and 16m/s. The results of SWIM beam 6 ° (a-d-g-j-m-p), beam 8 ° (b-e-h-k-n-q), and beam 10 ° (c-f-i-l-o-r) are all shown in the figure. The solid line in all the panels represent the mean omnidirectional wave height spectrum from the buoys under the sea surface conditions.

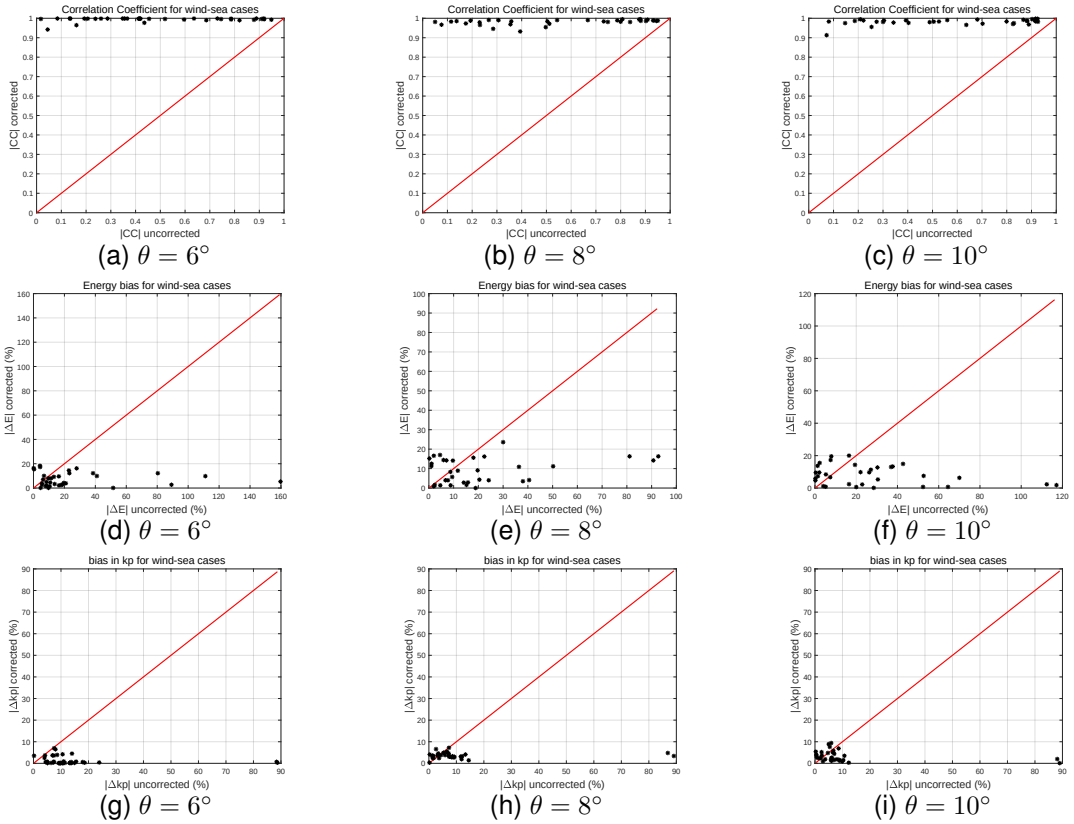

Fig. 3. Comparison of performance evaluation indicators of SWIM mean omnidirectional wave height spectrum before and after correction for the pure wind wave case. (a-b-c) shows the distribution of correlation coefficients, (d-e-f) integral energy error, and (g-h-i) relative peak wavenumber error for the three SWIM spectral beams.

is efficient.

B. Wave parameter H_s and T_{m-10} results

In order to better verify the correction effect of the correction network on SWIM omnidirectional wave height spectrum, the effective wave height H_s and energy wave period T_{m-10} are calculated based on each uncorrected and corrected SWIM omnidirectional wave height spectrum sample. Then SWIM uncorrected and corrected H_s and T_{m-10} are compared with MFWAM reanalyzed data matched in time and location. 1) and 2) compares the wave parameters for pure wind waves and for pure swells, respectively.

For SWIM , H_s is calculated by

$$H_s = 4\sqrt{\sum_{i=1}^{N} F(k_i)\Delta k_i}. \tag{12}$$

Where N is the point number of wave number, $F(k)$ is SWIM omnidirectional wave height spectrum.

The mean wave period T_{m-10} is calculated by:

$$T_{m-10} = m_{-1}/m_{0}. \tag{13}$$

$$m_n = \int_{f_{down}}^{f_{up}} f^n F(f) df. \tag{14}$$

Where $F(f)$ is the SWIM omnidirectional wave height spectrum in the frequency domain. Using the deep-water dispersion formula $\omega^2 = kg$, the conversion formula of $F(f)$ and $F(k)$ are as follows:

$$F(f)=F(k) \times \frac{8\pi^2 f}{g}. \tag{15}$$

f_{down}, f_{up} are the low and high frequency cutoff, respectively. As mentioned above, the wavenumber range of $k_{min} = 0.0056$ to $k_{max} = 0.306 rad/m$ are kept for SWIM omnidirectional wave height spectra, then correspondingly, $f_{down} = 0.037Hz$, $f_{up} = 0.28Hz$.

The MFWAM H_s and T_{m-10} are those provided in MFWAM reanalysis data files. The parameters are calculated within the frequencies range from 0.035 Hz to 0.58 Hz. Therefore, in the comparison of wave parameters below, it is necessary to consider that the frequency range corresponding to SWIM wave parameters and MFWAM wave parameters are slightly different.

1) Corrected H_s and T_{m-10} for the pure wind wave case: Fig.6 shows the comparison of SWIM and MFWAM H_s for the pure wind wave case. (a-b-c) and (d-e-f) correspond to the uncorrected and corrected SWIM H_s, respectively. (a-d) , (b-e) and (c-f) corresponds to SWIM beams 6°, 8° and 10°. The legend indicates the number of test sets (Num), correlation coefficient (abbreviated as CC), root-mean-square deviation (RMSE) and mean bias (MB), scattering index (SI) and fitting lines.

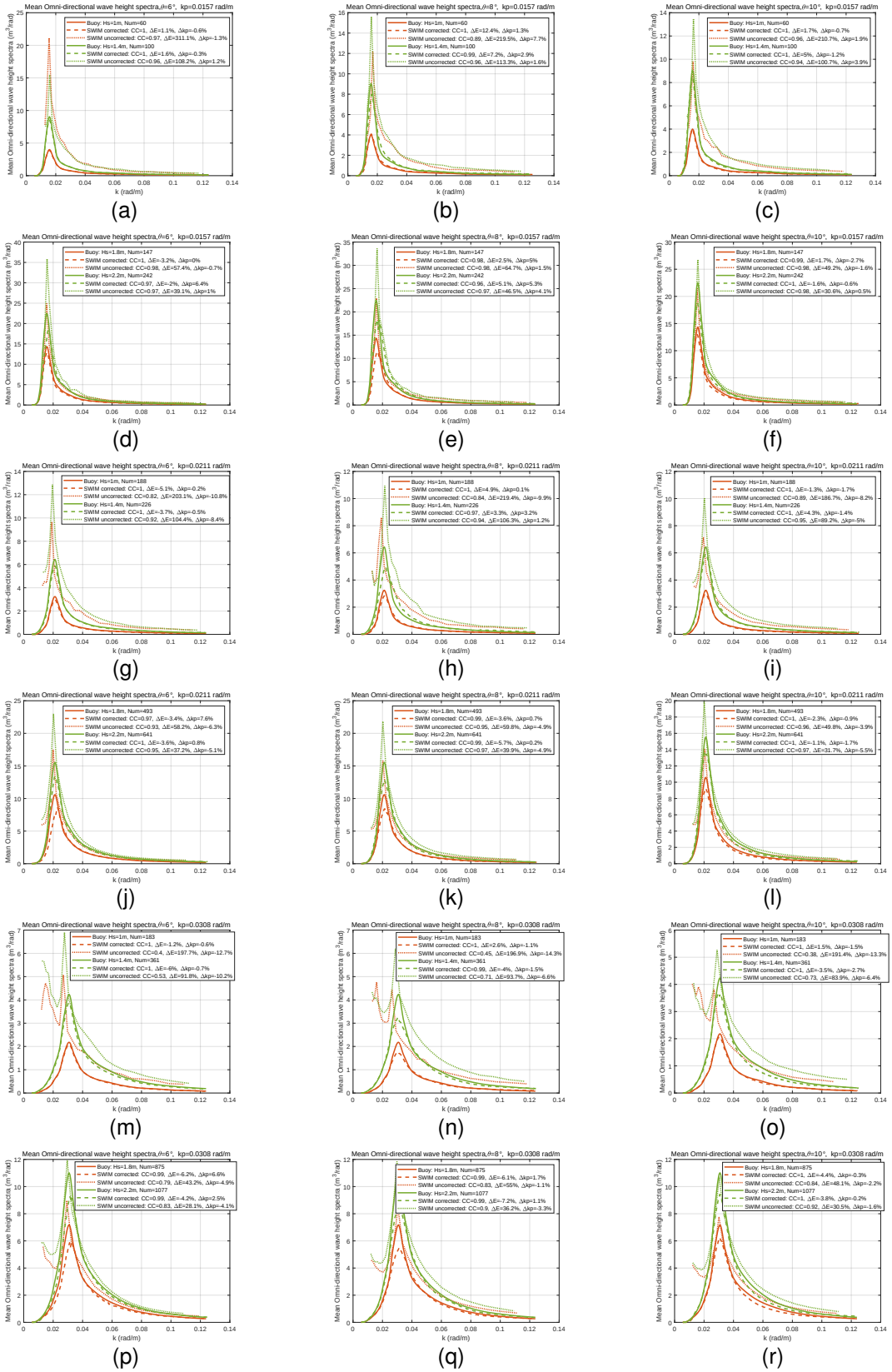

Fig. 4. Comparison of uncorrected and corrected SWIM mean omnidirectional wave height spectra for the pure swell case with the buoy mean omnidirectional wave height spectra when $k_p = 0.0157 rad/m$ (a-b-c-d-e-f), $k_p = 0.0211 rad/m$ (g-h-i-j-k-l), $k_p = 0.0308 rad/m$ (m-n-o-p-q-r). The red and green lines in Fig.4 (a-b-c-g-h-i-m-n-o) indicate significant wave heights of 1m and 1.4m, respectively; The red and green lines in Fig.4 (d-e-f-j-k-l-p-q-r) indicate significant wave heights of 1.8m and 2.2m, respectively. The results of SWIM beam 6 ° (a-d-g-j-m-p), beam 8 ° (b-e-h-k-n-q), and beam 10 ° (c-f-i-l-o-r) are shown in the figure.

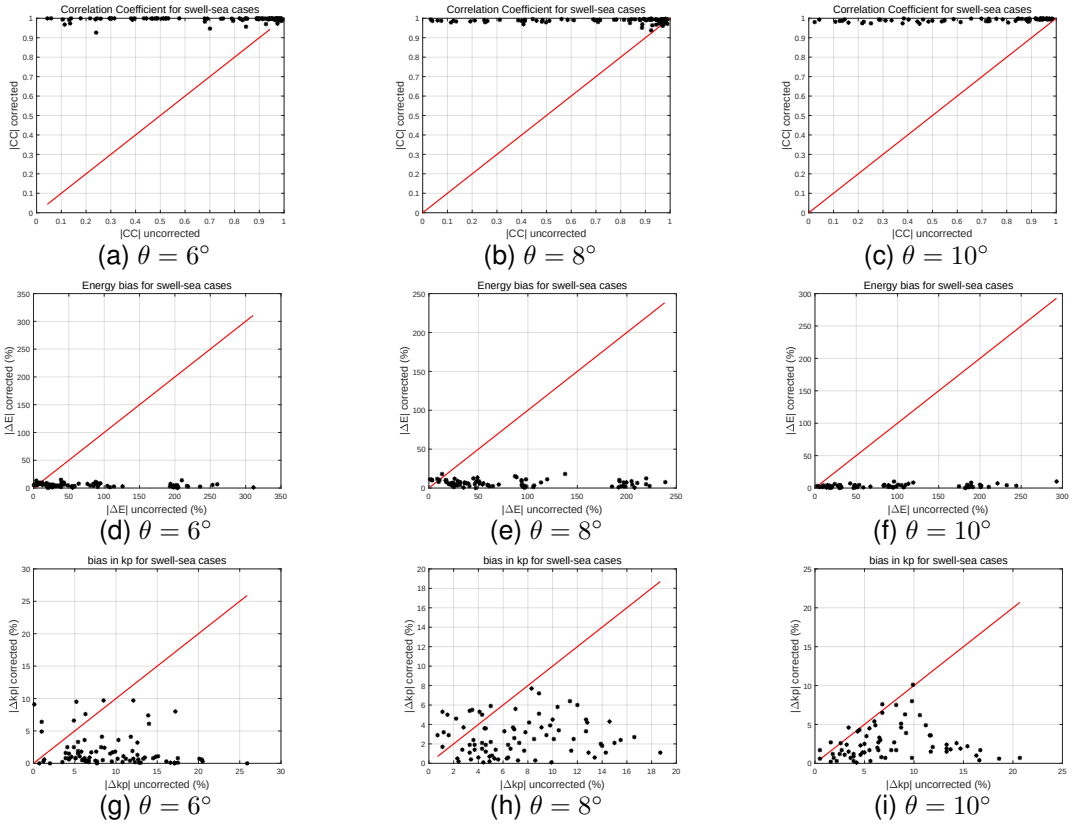

Fig. 5. Comparison of performance evaluation indicators of SWIM mean omnidirectional wave height spectrum before and after correction under swell sea. The arrangement of subfigures are as the same as those in Fig.3.

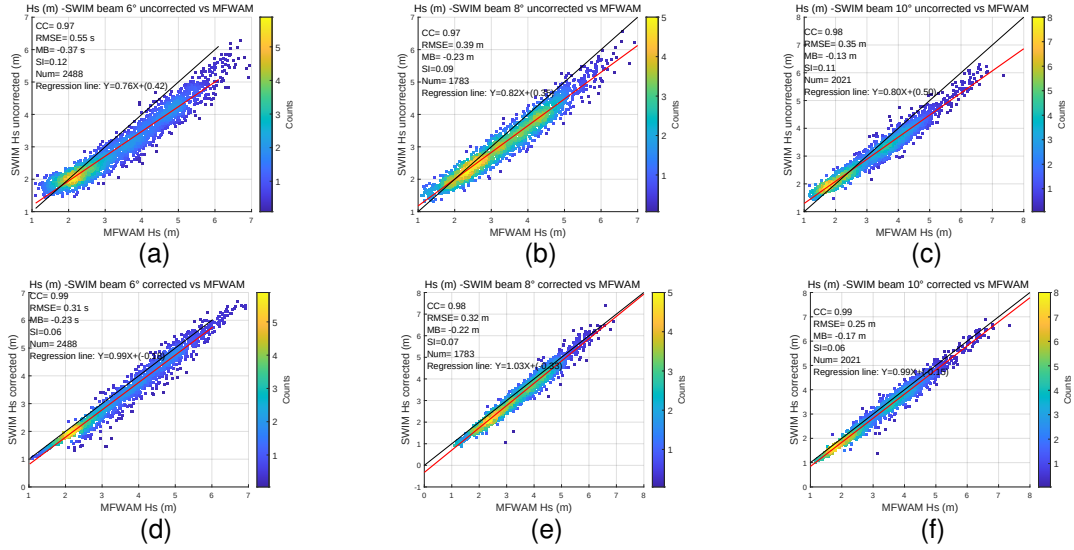

Fig. 6. Comparison of SWIM H_s (vertical axis) and MFWAM H_s (horizontal axis) for the pure wind wave case. (a-b-c) and (d-e-f) corresponds to the uncorrected and corrected SWIM H_s, respectively. （a-d）, (b-e) and (c-f) corresponds to SWIM beams 6°, 8° and 10°. In each panel the solid black line represents y=x. The red solid line represents the first-order fitting line of all scattered points.

From Fig.6 (a-b-c), it can be seen that for the pure wind wave case, compared to the H_s provided by MFWAM reanalysis data, uncorrected SWIM H_s for all beams are overestimated for H_s less than about 2 m, and underestimated for H_s larger than about 2 m. It is because that when H_s is small, the parasitic peaks at low wave numbers are more marked, causing an overestimation of the overall energy. As H_s increases, the influence of the parasitic peaks gradually weakens, while the energy loss caused by wave number truncation gradually increases. Since the frequency range for uncorrected SWIM H_s is 0.037-0.28Hz, however that for MFWAM H_s is 0.035-0.58Hz.

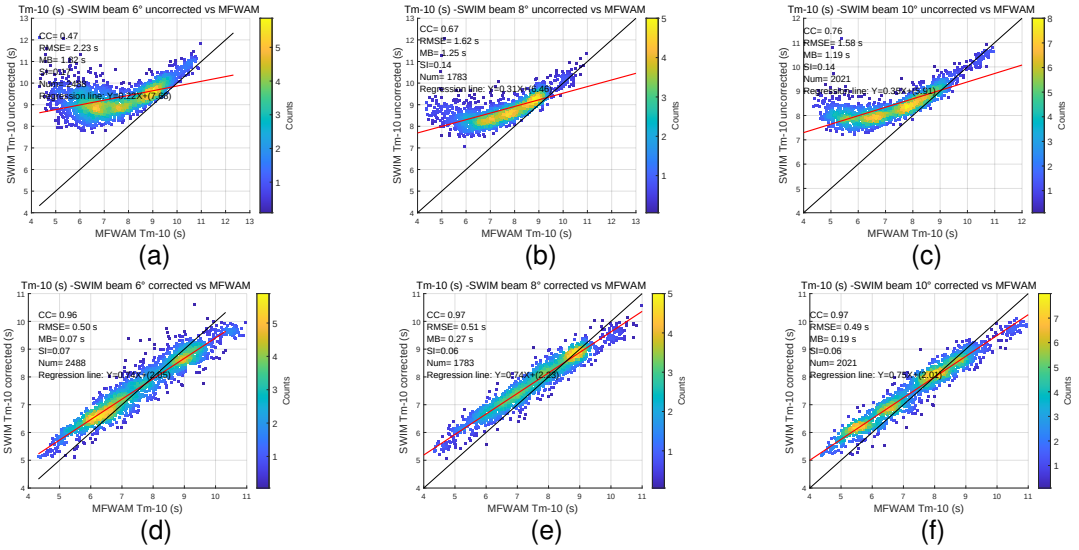

Fig. 7. Same as In Fig.6, but for T_{m-10}, for the pure wind wave case.

According to the comparison between Fig.6 (a-b-c) and (d-e-f), it can be seen that the correlation coefficients between corrected SWIM H_s for all beams and MFWAM H_s, as well as RMSE and the regression line, are better than that for the uncorrected. After correction, for SWIM beams 6 °, 8 ° and 10 ° , the CC increases to 0.99, 0.98, and 0.99, respectively; RMSE of the corrected SWIM H_s decreases from 0.55 m, 0.39 m and 0.35 m to 0.31 m, 0.32 m and 0.25 m; SI of the corrected decreases from 0.12, 0.09 and 0.11, to 0.06, 0.07 and 0.06, the slopes of the mean trend change from 0.76, 0.82 and 0.80 to 0.99, 1.03 and 0.99, respectively. A special case is that the MB of SWIM beam 10° Hs after correction is even worse than before correction. That is understandable because uncorrected H_s is overestimated when it is less than 2 m and underestimated when it is greater than 2 m, and the two cancel out, resulting in MB closer to 0.

The SWIM corrected Hs compared to that from MFWAM is slight underestimated in Fig. 6, the reason is not clear now. This indicates that although the established correction network has achieved good correction results, further optimization is still needed.

Fig.7 shows the comparison of SWIM and MFWAM mean wave period T_{m-10} for the pure wind wave case. From Fig.7(a-b-c) , compared with T_{m-10} provided by MFWAM reanalysis data, uncorrected T_{m-10} from SWIM 6°, 8°, 10° are overestimated when T_{m-10} is less than 9-10 s. As indicated by equation (13) and (14), T_{m-10} is more sensitive to low wave numbers. So, the parasitic peak occurring at low wave number in the uncorrected spectra of SWIM (see Fig.6) largely explains the overestimation of T_{m-10}.

From the comparison of Fig.7 (a-b-c) and (d-e-f), it can be seen that after correction, the performance of T_{m-10} has been greatly improved. This is mainly because the parasitic peaks at low wavenumber disappear in the corrected omnidirectional wave height spectra. The CC of corrected SWIM T_{m-10} for beams 6 °, 8 ° and 10 ° increases from 0.47, 0.67 and 0.76 to 0.96, 0.97, and 0.97, respectively; RMSE of the corrected T_{m-10} decreases from 2.23s, 1.62 s and 1.58 s to 0.50s, 0.51 s and 0.49 s, respectively; MB decreases from 1.82 s, 1.25 s and 1.19 s to 0.07 s, 0.27 s and 0.19 s, respectively; SI of the corrected T_{m-10} decreases from 0.17, 0.14 and 0.14, to 0.07, 0.06 and 0.06, respectively. It is also shown that the correction effect for SWIM beam 6 ° is the most significant.

2) Corrected H_s and T_{m-10} for swell sea: Fig.8 shows the comparison of SWIM and MFWAM H_s for the pure swell case. Fig.8 (a-b-c) shows that for the pure swell case, the uncorrected SWIM H_s for all beams are overestimated for H_s less than 3-3.5 m, and underestimated for H_s larger than 3-3.5 m, compared to the wave heights provided by the MFWAM reanalysis data. The specific reasons are the same as those explained in Fig.6.

According to the comparison between Fig.8 (a-b-c) and (d-e-f), it can be seen that the correlation coefficients between corrected SWIM H_s for all beams and MFWAM H_s, as well as RMSE, MB and the mean trend are better than those for the uncorrected cases. After correction, the CC of SWIM H_s for beams 6 °, 8 ° and 10 ° increases from 0.93, 0.93 and 0.95 to 0.98, 0.98, and 0.98, respectively; RMSE of the corrected SWIM H_s decreases from 0.35 m, 0.36 m and 0.33 m to 0.16 m, 0.16 m and 0.13 m, respectively; MB decreases from 0.22 m, 0.29 m and 0.26 m to -0.10 m, -0.10 m and 0.07 m, respectively; SI of the corrected decreases from 0.13, 0.10 and 0.10, to 0.06, 0.06 and 0.05; the slopes of the mean trend increase from 0.72, 0.78 and 0.74 to 0.98, 0.97 and 0.99, respectively.

Fig.8(d-e-f) also indicates that after correction the SWIM H_s for the pure swell cases remain underestimated compared to MFWAM values, for all SWIM beams. But compared to wind waves cases shown in Fig.6 (d-e-f), this underestimation has been reduced greatly.

Fig.9 shows the comparison of SWIM and MFWAM mean wave period T_{m-10} under swell sea. From Fig.9(a-b-c), compared with T_{m-10} provided by MFWAM reanalysis data,

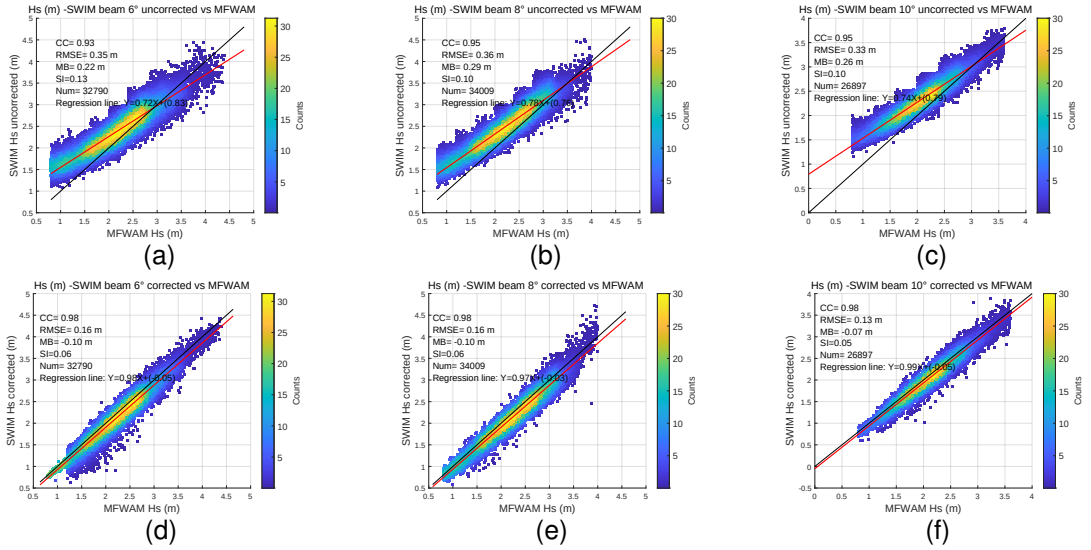

Fig. 8. Same as Fig.6, but for the pure swell cases.

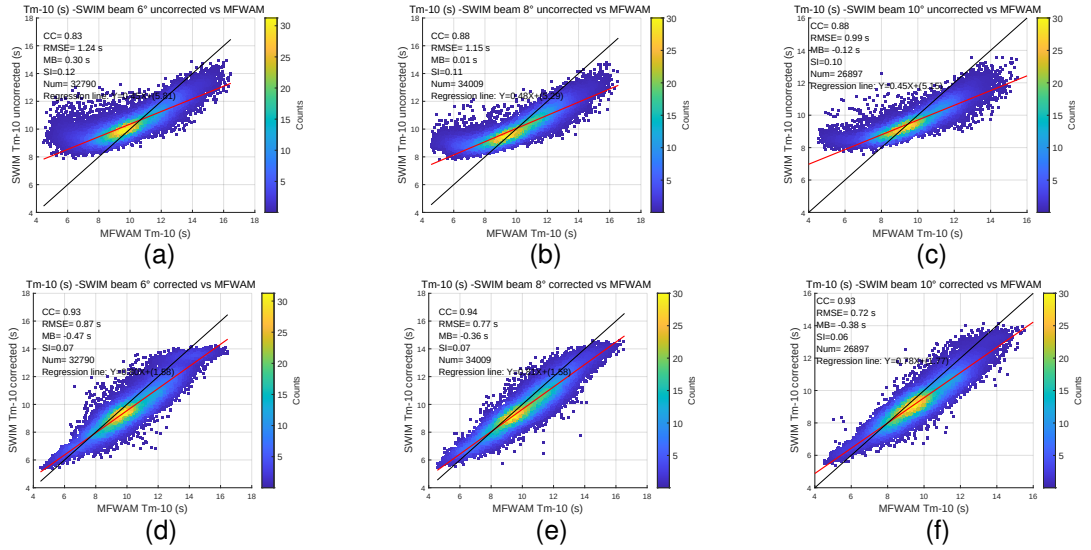

Fig. 9. Same as Fig. 7, but for cases of pure swell.

uncorrected T_{m-10} from SWIM (beams 6°, 8°, 10°) are overestimated when T_{m-10} is less than about 10 s. The specific reasons are the same as for Fig. 7 (a-b-c). When T_{m-10} is large, it is underestimated. This phenomenon mainly occurs in the sea conditions of high significant wave height, where SWIM omnidirectional wave height spectrum is less affected by parastic peak and surfboard effects.

By comparing Fig.9 (a-b-c) and (d-e-f), it can be seen that after correction, the performance of T_{m-10} for swell sea has been greatly improved. This is also mainly because the parasitic peaks at low wavenumber disappear in the corrected omnidirectional wave height spectra. The CC of corrected SWIM T_{m-10} for swell sea for 6 °, 8 °, and 10 ° beams increases from 0.83, 0.88 and 0.86 to 0.93, 0.94, and 0.93, respectively; RMSE of the corrected T_{m-10} decreases from 1.24s, 1.15 s and 0.99 s to 0.87s, 0.77 s and 0.72 s, respectively; SI of the corrected T_{m-10} decreases from 0.12, 0.11 and 0.10, to 0.07, 0.07 and 0.06, respectively. The slopes of the mean trend increase from 0.45, 0.48 and 0.45 to 0.80, 0.81 and 0.78, repectively.

From the comparison of Fig.9 and Fig.7, it is shown the correction effect on the wind wave cases is better than that on swell cases; this is because the correction network established has a good correction effect on the parasitic peak at low wave numbers in the omnidirectional spectra, and on the reduction of spectral value and left shift of spectral peak caused by surfboard effect, while spectra in wind wave situations are more subject to the above effects.

V. Conclusion

SWIM can provide global wave spectra, but under small sea conditions, the presence of parasitic peaks, nonlinear effects, and residual speckle noise leads to certain deviations between its wave spectra and those measured by buoys. Although some

studies have been done in correcting the integral parameters of SWIM wave spectra, no study was yet proposed on the correction of the wave spectra themselves.

Our work is focused on the correction of the omnidirectional wave height spectra of SWIM, by using the omnidirectional wave height spectra obtained by NDBC buoys as the reference. By defining the same sea state (wind wave/swell) and sea surface conditions (wind speed, peak wave number, and significant wave height), and using MFWAM reanalysis data to screen out the situation where a pure wave (wind/swell) dominates, a dataset matching NDBC buoys and SWIM wave spectra is obtained.

A convolution neural network (CNN) method based on U-Net was proposed for calibrating SWIM omnidirectional wave height spectra with NDBC buoy measurements. The corrected sea surface states are limited to the pure wind wave and pure swell case, and the corrected sea surface conditions are with H_s of 0.8m-4.2m, 0.8m-3.8m and 0.8m-3.4m, for SWIM beams 6, 8, 10°, respectively. In order to ensure that the SWIM omnidirectional wave height spectra under different sea surface conditions can be all corrected, data preprocessing methods are firstly developed, including dimensionless normalization of the SWIM omnidirectional wave height spectra by SWIM nadir H_s and weighted dimensionless normalization of the NDBC buoy mean omnidirectional wave height spectra by both SWIM nadir H_s and MFWAM H_s. According to the characteristics of omnidirectional wave height spectrum of SWIM, this paper proposes a weighted loss function with high wave number tail weighted penalty. Finally, a SWIM omnidirectional wave height spectrum correction network model based on BU-Net was established in this paper.

The calibration results show that the parasitic peak in the uncorrected SWIM omnidirectional wave height spectra appearing at low wavenumbers in the sea conditions mentioned above can be removed and the surfboard effect can be reduced. After correction, the correlation coefficients between the SWIM omnidirectional wave height spectra and the buoy are all greater than 0.90 for all the considered cases and all the SWIM beams, and the relative error of the peak wave number is within 10%. The relative error of the integrated energy is mostly less than 20% (H_s less than 10%).

In addition, the performance of spectral integrated parameters (effective wave height H_s, mean wave period T_{m-10}) calculated from omnidirectional wave height spectra for each spectral beam of SWIM has been verified using MFWAM reanalysis data. For the pure wind wave cases, and for the SWIM data from the beams 6 °, 8 °, and 10 °, the root mean square error of the corrected SWIM H_s decreases from 0.55 m, 0.39 m and 0.35 m to 0.31 m, 0.32 m and 0.25 m, respectively. For the same sea conditions, the root mean square error of the corrected T_{m-10} decreases from 2.23s, 1.62 s and 1.58 s to 0.50s, 0.51 s and 0.49 s, respectively. For the pure swell cases, the root mean square error of the corrected SWIM H_s decreases from 0.35 m, 0.36 m and 0.33 m to 0.16m, 0.16 m and 0.13 m, respectively. The root mean square error of the corrected T_{m-10} decreases from 1.24s, 1.15 s and 0.99 s to 0.87s, 0.77 s and 0.72 s, respectively. Thus, it is concluded that the correction effect on wind wave spectra is more important than that on swell spectra.

In summary, the correction network established from U-Net can be used for correcting SWIM omnidirectional wave height spectrum for pure wind wave and pure swell cases. By inputting the normalized SWIM beam 6° (8°, 10°) omnidirectional wave height spectrum by SWIM nadir H_s when H_s is 0.8m-4.2m (0.8m-3.8m, 0.8m-3.4m) into the established beam 6 ° (8°, 10°) correction network, then the outputs of the correction network are denormalized by SWIM nadir H_s, finally, the corrected omnidirectional wave height spectrum can be obtained with significant performance improvement.

As the initial stage of SWIM wave spectrum correction work, this work only studies the correction method of omnidirectional wave height spectrum. In the future, research on the correction of SWIM directional wave spectra will be carried out.

ACKNOWLEDGEMENT

The authors greatly appreciate the anonymous reviewers for their detailed comments that helped to improve the manuscript. The NDBC buoy data are available from the website of the National Centers for Environmental Information (https://www.ncei.noaa.gov/data/oceans/ndbc/cmanwx/).
The SWIM data is available from the "Aviso+" website (https://www.aviso.altimetry.fr/en/data/products/wind/wave-products/wave-wind-cfosat-products.html).The MFWAM data are available from the Copernicus Marine Environment Monitoring Service (CMEMS) (https://marine.copernicus.eu).

REFERENCES

[1] F. Ardhuin et al., "Observing sea states," Frontiers Mar. Sci., vol. 6, p. 124, Apr. 2019, doi: 10.3389/fmars.2019.00124.

[2] W. R. Alpers, D. B. Ross, and C. L. Rufenach, "On the detectability of ocean surface waves by real and synthetic aperture radar," J. Geophys. Res., vol. 86, no. C7, p. 6481, 1981, doi: 10.1029/JC086iC07p06481.

[3] K. Hasselmann and S. Hasselmann, "On the nonlinear mapping of an ocean wave spectrum into a synthetic aperture radar image spectrum and its inversion," J. Geophys. Res., vol. 96, no. C6, p. 10713, Nov. 1991, doi: 10.1029/91JC00302.

[4] F. C. Jackson, "An Analysis of short pulse and dual frequency radar techniques for measuring ocean wave spectra from satellites," Radio Sci., vol. 16, no. 6, pp. 1385–1400, Nov. 1981, doi: 10.1029/RS016i006p01385.

[5] D. Hauser et al., "New Observations from the SWIM Radar On-Board CFOSAT: Instrument Validation and Ocean Wave Measurement Assessment," IEEE Trans. Geosci. Remote Sens., vol. 59, no. 1, pp. 5–26, 2021, doi: 10.1109/TGRS.2020.2994372.

[6] E. Le Merle et al., "Directional and Frequency Spread of Surface Ocean Waves From SWIM Measurements," J. Geophys. Res. Ocean., vol. 126, no. 7, 2021, doi: 10.1029/2021JC017220.

[7] G. Liang, J. Yang, and J. Wang, "Accuracy Evaluation of CFOSAT SWIM L2 Products Based on NDBC Buoy and Jason-3 Altimeter Data," Remote Sens., vol. 13, no. 5, p. 887, Feb. 2021, doi: 10.3390/rs13050887.

[8] H. Jiang, A. Mironov, L. Ren, A. V. Babanin, J. Wang, and L. Mu, "Validation of Wave Spectral Partitions From SWIM Instrument On-Board CFOSAT Against In Situ Data," IEEE Trans. Geosci. Remote Sens., vol. 60, pp. 1–13, 2022, doi: 10.1109/TGRS.2021.3110952.

[9] Ying Xu, Danièle Hauser, Jianqiang Liu, Jianyang Si, Chen Yan, Shufen Chen, Junmin Meng, Chenqing Fan, Meijie Liu, Ping Chen: Statistical Comparison of Ocean Wave Directional Spectra Derived From SWIM/CFOSAT Satellite Observations and From Buoy Observations. IEEE Trans. Geosci. Remote. Sens. 60: 1-20 (2022).

[10] E. Peral, E. Rodríguez, and D. Esteban-Fernández, "Impact of surface waves on SWOT's projected ocean accuracy," Remote Sens., vol. 7, no. 11, pp. 14509–14529, 2015, doi: 10.3390/rs71114509.

[11] Wang J K , Aouf L , Dalphinet A , et al. Acquisition of the Significant Wave Height From CFOSAT SWIM Spectra Through a Deep Neural Network and Its Impact on Wave Model Assimilation[J]. Journal of Geophysical Research: Oceans, 2021, 126(6).
[12] Bo Li, Junmin Li, Junliang Liu, Shilin Tang, Wuyang Chen, Ping Shi, Yupeng Liu: Calibration Experiments of CFOSAT Wavelength in the Southern South China Sea by Artificial Neural Networks. Remote. Sens. 14(3): 773 (2022).
[13] Jiang Haoyu, Song Yuhao, Mironov Alexey, Yang Zheng, Xu Ying, Liu Jianqiang. Accurate mean wave period from SWIM instrument on-board CFOSAT[J]. Remote Sensing of Environment,2022,280.
[14] G. Huffman, D. Bolvin, D. Braithwaite, K. Hsu, and R. Joyce, "NASA Global Precipitation Measurement (GPM) Integrated Multi-satellitE Retrievals for GPM (IMERG)," Nasa, no. December, p. 29, 2019, [Online].
[15] D. Hauser, C. Tison, T. Amiot, L. Delaye, N. Corcoral, and P. Castillan, "SWIM: The First Spaceborne Wave Scatterometer," IEEE Trans. Geosci. Remote Sens., vol. 55, no. 5, pp. 3000–3014, 2017, doi: 10.1109/TGRS.2017.2658672.
[16] C. Tourain et al., "Benefits of the Adaptive Algorithm for Retracking Altimeter Nadir Echoes: Results From Simulations and CFOSAT/SWIM Observations," IEEE Trans. Geosci. Remote Sens., vol. 59, no. 12, pp. 9927–9940, Dec. 2021, doi: 10.1109/TGRS.2021.3064236.
[17] NDBC Web Data Guide, "NDBC Web Data Guide," Stennis Space Center, 2015.
[18] F. Ardhuin et al., "Semiempirical dissipation source functions for ocean waves. Part I: Definition, calibration, and validation," J. Phys. Oceanogr., vol. 40, no. 9, pp. 1917–1941, 2010.
[19] X. Chu, Y. He, and G. Chen, "Asymmetry and Anisotropy of Microwave Backscatter at Low Incidence Angles," IEEE Transactions on Geoscience & Remote Sensing, vol. 50, pp. 4014-4024.
[20] D. Hauser, G. Caudal, S. Guimbard, and A. Mouche, "Reply to comment by Paul A. Hwang on 'A study of the slope probability density function of the ocean waves from radar observations' by D. Hauser et al.," J. Geophys. Res., vol. 114, no. C2, p. C02009, Feb. 2009, doi: 10.1029/2008JC005117.
[21] D. Sun, W. Huang, Y. Luo, J. Luo, J. S. Wright, H. Fu, et al. A Deep Learning-Based Bias Correction Method for Predicting Ocean Surface Waves in the Northwest Pacific Ocean. Geophysical Research Letters. 2022, 46(23): e2022GL100916.
[22] C. Tison, D. Hauser, and P. Castillan, "Swim products usersguide," Centre National d'Etudes Spatiales, Toulouse, France, 2019.[Online].
[23] Xu J., et al."Reluplex made more practical: Leaky ReLU." Proceedings - IEEE Symposium on Computers and Communications 2020-July.(2020). doi:10.1109/ISCC50000.2020.9219587.